Dynamics of Noncovalent Supramolecular Complexes. NMR Study of the Rotational Barriers in Chiral BINAP Palladium(II) and Platinum(II) Bis(phosphane) Complexes That Resemble the Minimal Subunits of Chiral Polygons and Polyhedra

Martin Fuss and Hans-Ullrich Siehl*

Department of Organic Chemistry I, Universität Ulm, 89069 Ulm, Germany

Bogdan Olenyuk and Peter J. Stang*

Department of Chemistry, The University of Utah, Salt Lake City, Utah 84112

Received May 18, 1998

In the reaction between 3-picoline, 2-bromo-5-methylpyridine, 2-methylquinoline, 3-methylisoquinoline, and [M(*R*-(+)-BINAP)][OTf]$_2$ (M = Pd, Pt; BINAP = 2,2′-bis(diphenylphosphino)-1,1′-binaphthyl), the nature and the distribution of the products were investigated by various physical and spectroscopic methods. The α-substituents on the heteroaryl ring, such as the bromine atom in 2-bromo-5-methylpyridine or the methyl group in 2-methylquinoline, tend to promote the simultaneous formation of mono(heteroaryl)- and bis(heteroaryl)-containing products. The reaction of the most sterically demanding 2-methylquinoline favors the formation of mono(heteroaryl) complexes exclusively within the limits of NMR detection. Reaction of 3-picoline with the chiral Pd(II) and Pt(II) bis(triflates) results in the formation of diastereomeric, square-planar, cationic complexes, due to the hindered rotation about the metal−nitrogen heteroaryl bond. ^{1}H NMR variable-temperature studies of [M(*R*-(+)-BINAP)(3-picoline)$_2$][OTf]$_2$ were performed. The activation barriers for the rotation of the *β*-picoline ligands around the M−N linkage axis were determined for [Pd(*R*-(+)-BINAP)(3-picoline)$_2$][OTf]$_2$ and [Pt(*R*-(+)-BINAP)(3-picoline)$_2$][OTf]$_2$ by a kinetic line shape analysis of the methyl signals. The Gibbs free energy of activation was found to be 12(±0.5) kcal/mol for the Pd complex **15** and 14(±0.5) kcal/mol for the Pt complex **16**. *Ab initio* calculations (HF/lanl2dz) of model complexes [dpe]Pd(HN=CH$_2$)$_2^{2+}$ and [dpe]Pt(HN=CH$_2$)$_2^{2+}$ (dpe = diphosphinoethylene) provided insights into the observed results. The nitrogen−metal *π*−*σ*-interaction is found to be stronger for the Pt complex, resulting in a higher energy barrier for the rotation around the Pt−N bond compared to the rotation around the Pd−N bond. A comparison is made between the covalent and coordinated Pt(II) complexes, and the similarities and differences of their dynamic behavior are discussed.

Introduction

Transition-metal-mediated self-assembly and metal−ligand interactions are becoming increasingly popular in the construction of a variety of nanoscale-sized entities. The basic appeal of this method is in its highly convergent synthetic protocol, the fast and facile formation of the final product, as such metal−donor ligand interactions are established very rapidly, and most importantly, the great versatility of this method, as a large number of nanostructures can be prepared *via* the combination of a relatively small number of building blocks.[1] Recently, the application of this principle has been demonstrated in the self-assembly of discrete metallacyclic polygons and polyhedra.[2] Among these assemblies, chiral structures **1**−**5** (Chart 1) occupy an important place, as they are the first examples of transition-metal-based discrete supramolecular assemblies with controlled stereochemistry. Investigation of the chemistry of these chiral noncovalent assemblies provides insights into topological isomerism as well as the important principles of stereocontrolled self-assembly. Although a full understanding of these aspects is a complex task, a first step is the careful determination of rotational barriers and a detailed study of the

(1) Robson, R.; Abrahams, B. F.; Batten, S. R.; Gable, R. W.; Hoskins, B. F.; Liu, J. In *Supramolecular Architecture;* ACS Symposium Series 499; Bein, T., Ed.; American Chemical Society: Washington, DC, 1992; Chapter 19. Chambron, J.-C.; Dietrich-Buchecker, C.; Sauvage, J.-P., Transition Metals as Assembling and Templating Species. In *Comprehensive Supramolecular Chemistry;* Lehn, J.-M., Chair Ed.; Atwood, J. L., Davis, J. E. D., MacNicol, D. D., Vögtle, F., Exec. Eds.; Pergamon Press: Oxford, U.K., 1996; Vol. 9, Chapter 2, p 43. Baxter, P. N. W. Metal Ion Directed Assembly of Complex Molecular Architectures and Nanostructures. In *Comprehensive Supramolecular Chemistry;* Lehn, J.-M., Chair Ed.; Atwood, J. L., Davis, J. E. D., MacNicol, D. D., Vögtle, F., Exec. Eds.; Pergamon Press: Oxford, U.K., 1996; Vol. 9, Chapter 5, p 165. Constable, E. C. Polynuclear Transition Metal Helicates. In *Comprehensive Supramolecular Chemistry;* Lehn, J.-M., Chair Ed.; Atwood, J. L., Davis, J. E. D., MacNicol, D. D., Vögtle, F., Exec. Eds.; Pergamon Press: Oxford, U.K., 1996; Vol. 9, Chapter 6, p 213.

(2) Stang, P. J.; Olenyuk, B. *Acc. Chem. Res.* **1997**, *30*, 502.

10.1021/om9803927 CCC: $18.00
Publication on Web 01/27/1999

Chart 1. Chiral Nanoscopic Assemblies and Their Minimal Subunits

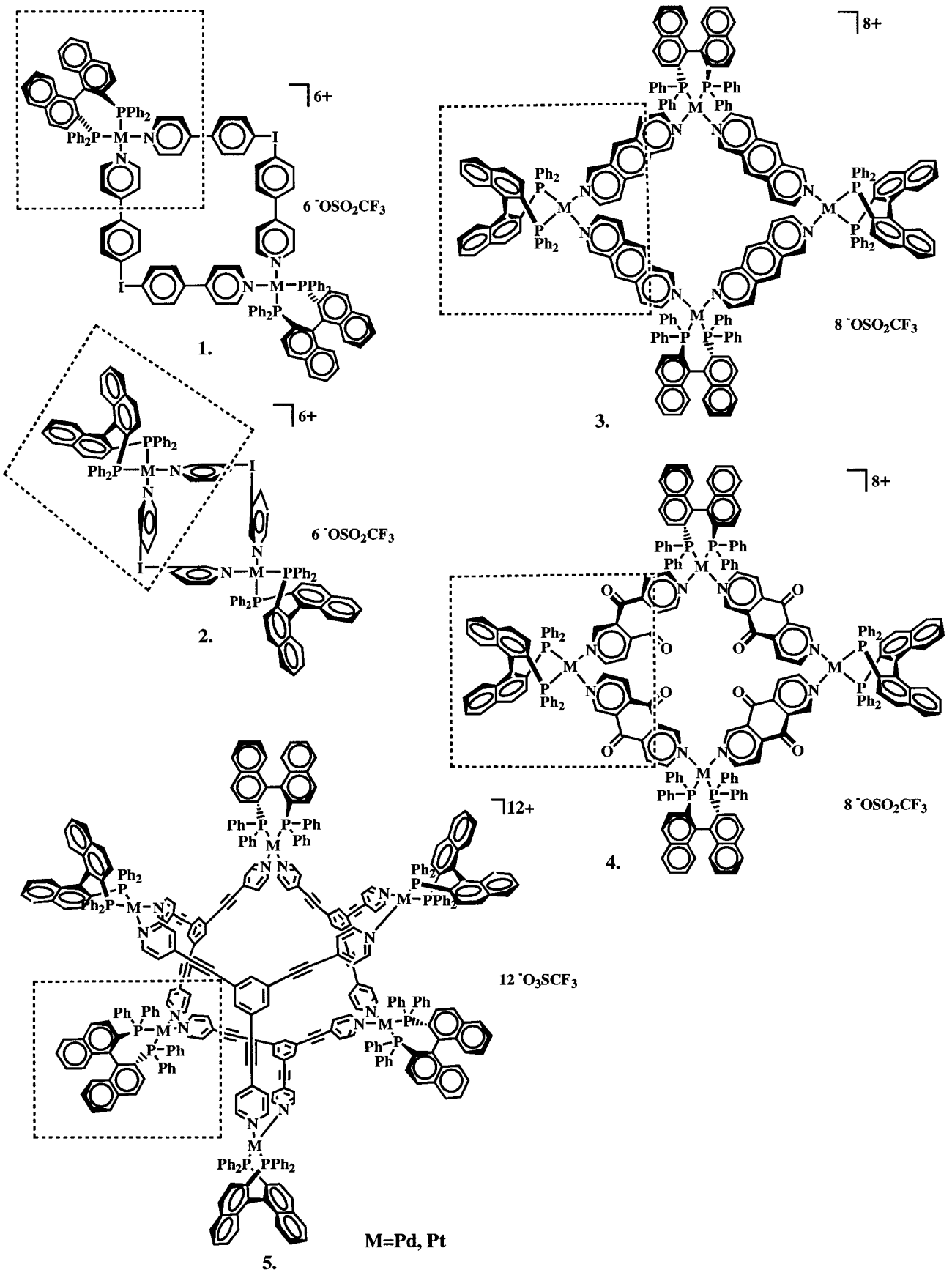

fluxional behavior of various heteroaryl complexes of Pd(II) and Pt(II) bis(phosphanes), as they are directly responsible for the existence of different rotational isomers in these chiral assemblies. Chiral BINAP Pd and Pt coordination complexes are subunits of chiral assemblies **1**−**5** and others.[3] As examples of chiral

Chart 2

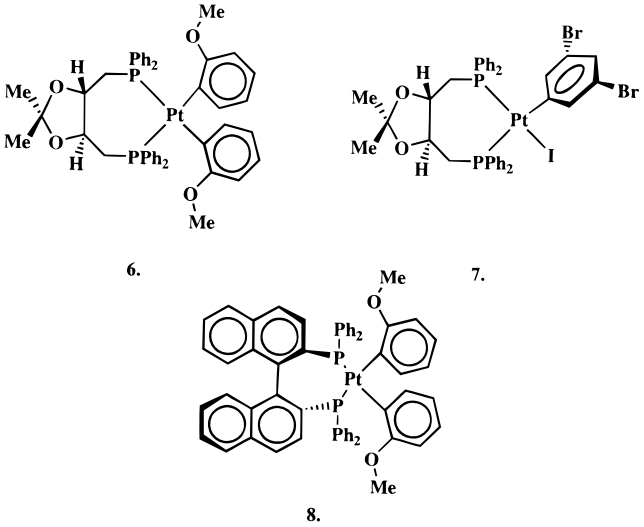

covalent Pt complexes such as compounds **6**−**8** (Chart 2) have been reported in the literature,[4] it is also of interest to compare the rotational barriers between the covalent Pt and Pd complexes and coordination complexes with the weaker metal−heteroaryl bond.

Results and Discussion

Synthesis and NMR Studies of Cationic Heteroaryl Complexes of *R*-(+)-BINAP Pt(II) and Pd(II) Bis(phosphanes). We chose the chiral *R*-(+)-2,2′-bis(diphenylphosphino)-1,1′-binaphthyl (*R*-(+)-BINAP)[5] metal triflates for the preparation of the desired complexes in the form of their stable monohydrates **9** and **10** as an alternative to the highly hygroscopic anhydrous bis(triflates).[6,7] Upon simple addition of these triflates to an excess of the appropriate heterocycle in dichloromethane solution complexes **11**−**14** were prepared in good isolated yields (Scheme 1). Complexes **15**−**18** were prepared *via* a similar procedure (Scheme 2).

At room temperature both bis(phosphane) 2-bromo-5-methylpyridine complexes **11** and **12** show a set of distinct peaks for the methyl group in the high-field region of the ^{1}H NMR spectra, indicating that several isomers and/or compounds were formed. In the ^{31}P NMR spectrum the signals are located in two different regions. For Pd complex **11**, one set is centered around 24−26 ppm, corresponding to the two indistinguishable *anti* isomers (diastereomeric pair) **11a,b** and the *syn* (*meso*) complex **11c**, along with a singlet at 32 ppm, which corresponds to complex **11d** with only one heteroaryl coordinated to the transition metal. This hypothesis is confirmed by analysis of the high-field region of the ^{1}H NMR spectra. Integration of these signals and comparison of their intensity with the intensity of the BINAP naphthalene signals indicates a 3:2 ratio, corresponding to the complex with only one heterocyclic ligand. Examination of the spectra of complex **12** reveals a similar trend; however, the ratio of disubstituted to monosubstituted complex is somewhat higher, allowing for the separation of the disubstituted products **12a**−**c** from the heteroaryl complex **12d**. The second valence of each transition metal is occupied by a labile weakly coordinated anion, such as water or triflate,[6] and since the equilibration between the metal and this ligand is very fast on the NMR time scale, the monosubstituted complex exhibits only a singlet in the ^{31}P NMR spectra. Similar averaging is observed in the ^{31}P NMR spectra for the monohydrate complexes of BINAP−Pd(II) and BINAP−Pt(II) bis(triflates).[3,7]

Interestingly, complexes **13** and **14** each exhibit only a single signal in the methyl region and a sharp singlet in the phosphorus NMR spectrum. These signals are unchanged when the sample is either cooled or heated; therefore, they must not be the time-averaged signals of several isomeric bis(heteroaryl) complexes. Integration of the methyl signal and comparison of its intensity to the intensities of various BINAP protons indicates the almost exclusive formation of the respective monosubstituted complexes. Apparently, with the bulkier 2-methylquinoline complexes the steric interference of

Scheme 1

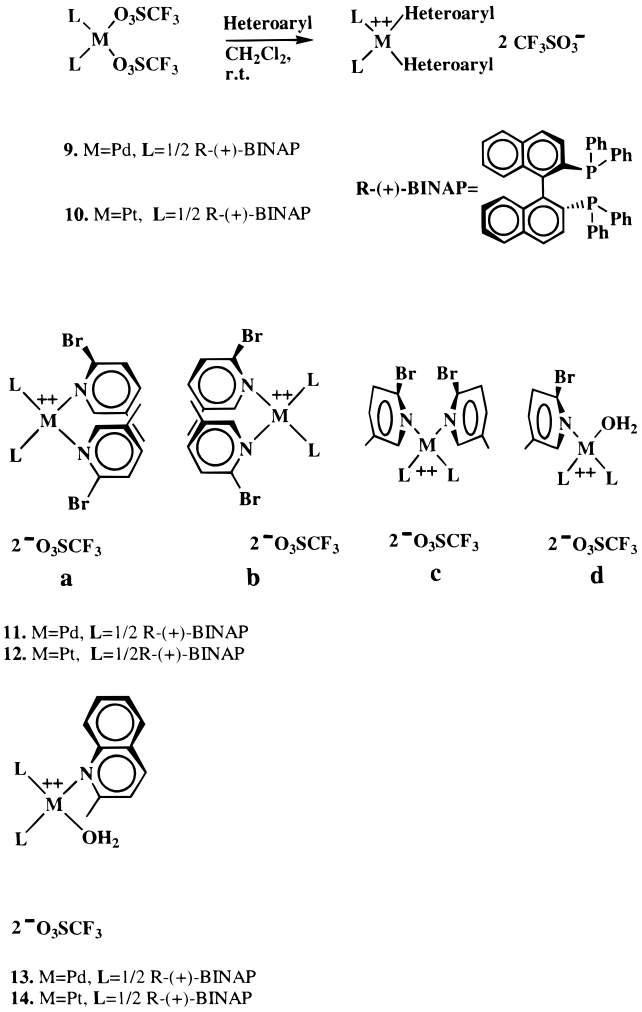

(3) Olenyuk, B.; Whiteford, J. A.; Stang, P. J. *J. Am. Chem. Soc.* **1996**, *118*, 8221. Stang, P. J.; Olenyuk, B. *Angew. Chem., Int. Ed. Engl.* **1996**, *35*, 732. Stang, P. J.; Olenyuk, B.; Muddiman, D. C.; Smith, R. D. *Organometallics* **1997**, *16*, 3092.

(4) Brown, J. M.; Pérez-Torrente, J. J.; Alcock, N. W. *Organometallics* **1995**, *14*, 1195. Alcock, N. W.; Brown, J. M.; Pérez-Torrente, J. J. *Tetrahedron Lett.* **1992**, *33*, 389.

(5) Takaya, H.; Mashima, K.; Koyano, K.; Yagi, M.; Kumobayashi, H.; Taketomi, T.; Akutagawa, S.; Noyori, R. *J. Org. Chem.* **1986**, *51*, 629. Miyashita, A.; Yasuda, A.; Takaya, H.; Torimi, K.; Ito, T.; Souchi, T.; Noyori, R. *J. Am. Chem. Soc.* **1980**, *102*, 7932.

(6) Lawrance, G. A. *Chem. Rev.* **1986**, *86*, 17.

(7) Stang, P. J.; Olenyuk, B.; Arif, A. M. *Organometallics* **1995**, *14*, 5281.

Scheme 2

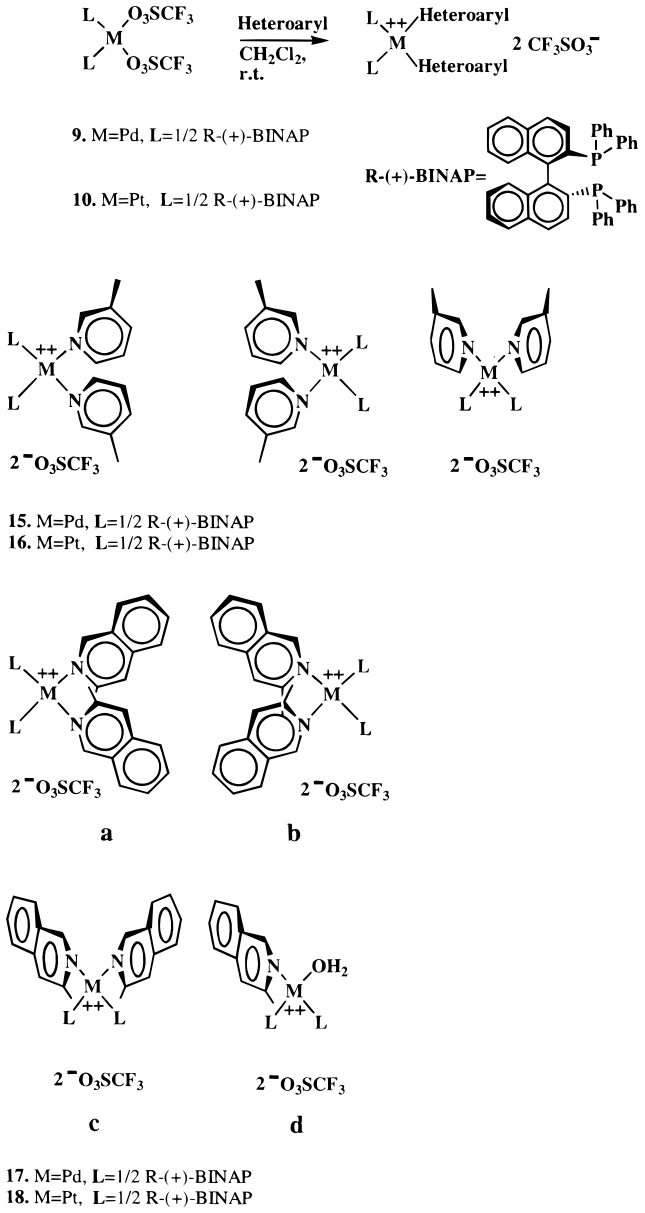

the nearby methyl group is reinforced by the influence of the annelated benzene ring, especially of its H-8 hydrogen. Since the methyl group and H-8 of the quinoline are located along the axis perpendicular to the transition-metal coordination plane (Figure 1), they are capable of blocking the subsequent access of a second nucleophile with remarkable efficiency. Our analysis of the NMR spectra indicates that the remaining transition-metal valence is occupied by a water molecule.

When the methyl group is located further away from the transition-metal center as in complexes **15** and **16**, very little or no steric influence on the stoichiometry is observed and both **15** and **16** are readily formed as disubstituted complexes. Variable-temperature NMR investigation of **15** and **16** indicated a change of the dynamic process from the slow to the fast exchange limit using the picoline methyl substituents as reporter groups, within an observable temperature range, thereby making complexes **15** and **16** suitable for further determination of the rotation barriers. Our preliminary observations[7] and literature data[11] suggest that the value of the rotational barriers in these Pd- and Pt-containing complexes is governed by at least two factors: steric effects of the BINAP ligand and electronic factors which are dominant in complexes that contain heteroaryls with a high dipole moment.

NMR investigation of the BINAP−Pd(3-methylisoquinoline) complex **17** indicates behavior similar to that of complex **11**, except that the ratio of disubstituted products **17a**−**c** to monosubstituted complex **17d** is somewhat higher. For Pt complex **18**, however, this ratio seems to be reversed, thereby favoring the formation of monosubstituted product, which can be separated from the mixture by recrystallization and then characterized.

Determination of the Rotational Barriers.[9] Under conditions of slow exchange, the methyl groups of [Pd(*R*-(+)-BINAP)(3-picoline)$_2$][OTf]$_2$ (**15**) and [Pt(*R*-(+)-BINAP)(3-picoline)$_2$][OTf]$_2$ (**16**) give a series of isolated singlets for the methyl groups at about 2 ppm, serving as a good probe for the conformational analysis of these complexes. At $T = -51$ °C, complexes **15** and **16** each show four distinct signals for the methyl groups in the proton NMR spectrum. These signals are assigned to the three conformers A−C (Scheme 3). Conformers A and B are each C_2-symmetric diastereomers. Rotation around the C_2 axis superimposes the two methyl groups in A and B, and hence, only one NMR signal is observed for the methyl protons of A (δ_A 2.015 ppm for **15** and δ_A 2.059 ppm for **16**) and likewise one signal for the methyl protons of B (δ_B 1.915 ppm for **15** and δ_B 1.913 ppm for **16**) (Figure 2). The different intensities of the signals reveal the different thermodynamic stabilities of isomers A and B. However, since the identity of the two conformers could not be determined from the NMR spectra alone because there is no easy way to assign the signals to the isomers by NOESY or ROESY NMR experiments, the assignment of the two signals δ_A and δ_B to the two conformers A and B is arbitrary. Since conformer C has no symmetry elements higher than C_1, the methyl protons on the left and on the right picoline ligand are diastereotopic due to the chiral BINAP ligand. Hence, they show up in the ^{1}H NMR spectrum as two different signals of equal intensity, (δ_C 1.981 ppm and δ_C 1.880 ppm for **15** and δ_C 2.029 ppm and δ_C 1.891 ppm for **16**). These four signals of Pd complex **15** as well as of Pt complex **16** each average to one signal upon warming of the samples (Figure 2).

The set of four methyl signals seen under conditions of slow exchange at low temperatures for each complex **15** and **16** is averaged to one single peak under conditions of fast exchange above −13 °C for **15** and +32 °C for **16**. The exchange processes shown in Scheme 4 explain the temperature-dependent line shapes of the

(8) The line shape analysis was performed using the WIN-DYNAMICS program: Bruker-Franzen Analytic GmbH and Ilyasov, K.; Nedopekin, O.; Version 1.0, *β*-950312.

(9) Sandström, J. *Dynamic NMR Spectroscopy*; Academic Press: New York, 1982.

(10) See Chapter 7 in ref 9.

(11) For examples of restricted rotation about Pd−aryl, Pt−aryl, or Ni−aryl bonds, see: Wada, M.; Sameshima, K. *J. Chem. Soc., Dalton Trans.* **1981**, 240. Gritffits, D. B.; Young, G. B. *Organometallics* **1986**, *5*, 1744. Baumgärtner, R.; Brune, H. A. *J. Organomet. Chem.* **1988**, *350*, 115. Anderson, G. K.; Cross, R. J.; Manojlovic-Muir, L.; Muir, K. W.; Rocamora, M. *Organometallics* **1988**, *7*, 1520. Alster, P. L.; Boersma, J.; Smeets, W. J. J.; Spek, A. L.; van Koten, G. *Organometallics* **1993**, *12*, 1639.

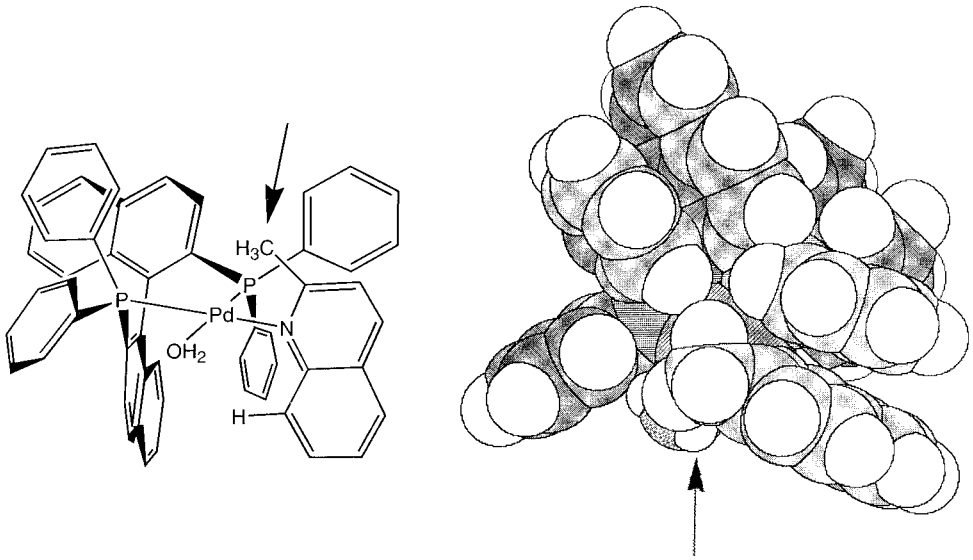

Figure 1. Structural formula (left) and space-filling model (right) of the cationic portion of [Pd(*R*-(+)-BINAP)(2-methylquinoline)(H_2O)][OTf]$_2$ (**13**), derived from the MM2 force field calculations. The top view is perpendicular to the Pt coordination plane. The quinoline methyl group, as indicated by the arrow, is located directly above the coordination plane of the palladium atom.

Scheme 3

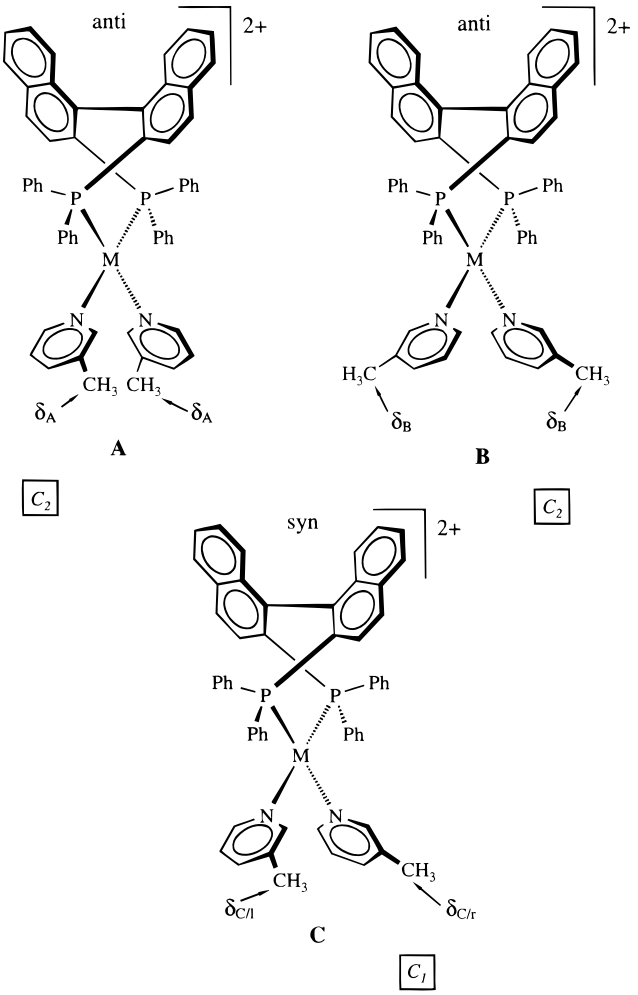

^{1}H NMR methyl signals of **15** and **16** (Figures3 and 4). The exchange scheme allows the interconversion of conformers A and C and of conformers B and C by rotation of either the left or the right β-picoline ligand. Due to these processes the chemical shift δ_A of conformer A is averaged with the chemical shifts $\delta_{C/r}$ and $\delta_{C/l}$ of conformer C. Likewise, the chemical shift δ_B of B is averaged with the chemical shifts $\delta_{C/r}$ and $\delta_{C/l}$ of C. Regarding only this stepwise interconversion of C to C *via* A and B, the simulation of the experimental methyl ^{1}H NMR signals within the fast exchange limit leads to two separate signals in contrast to one single averaged signal observed for **15** as well as for **16**. For the correct simulation of the experimental spectra in the fast exchange region a one-step degenerate interconversion of C averaging the chemical shifts $\delta_{C/r}$ and $\delta_{C/l}$ has to be included.

The direct averaging of $\delta_{C/r}$ and $\delta_{C/l}$ might in principle be due to a conformational change of the bis(phosphino)-metallacycloheptadiene moieties of **15** and **16** leading to racemization of the complexes. Neither the Pd complex **15** nor the Pt complex **16** changes the sign of optical rotation upon warming to reflux and cooling in methanol or nitromethane. Thus, a conformational change of complexes **15** and **16** involving the BINAP ligand can be excluded. The direct averaging of $\delta_{C/r}$ and $\delta_{C/l}$ could be caused, however, by the degenerate one-step interconversion of conformer C due to a concerted rotation of both picoline ligands. This degenerate, one-step interconversion can also be caused by the fast but nonconcerted double-flip of the two pyridine rings that is becoming apparent at these elevated temperatures. When this process becomes faster than the NMR time scale, it is not possible to distinguish the four separate interconversions, only their aggregate A−B and C−C interconversions.

The simulation of the spectra[8] allowing this double-flip process leads to good agreements with the experimental spectra (Figures 3 and 4) in the slow as well as in the fast exchange region. The activation barrier for the interconversion of conformer C by a concerted rotation of the picoline ligands is higher than the energy barrier determined for the rotation of a single picoline. The rate constants (k_{AC}, k_{CA}, k_{BC}, k_{CB}, k_{CC}) determined by the simulation of the spectra are given in Figures 3 and 4.

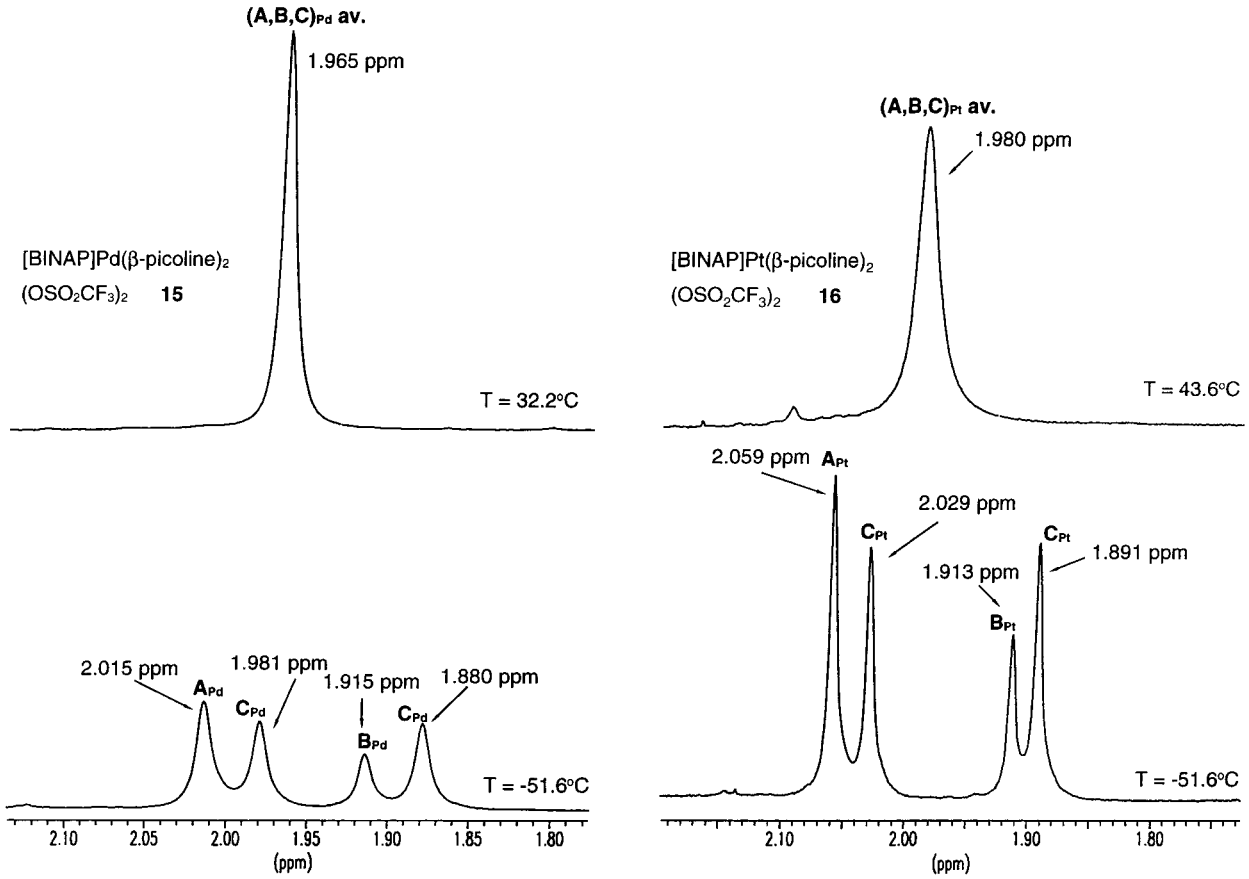

Figure 2. 400 MHz ^{1}H NMR spectra of complexes **15** (left) and **16** (right) at various temperatures (solvent CD_3OD; δ-(CHD_2OD) 3.31 ppm).

In accord with the exchange scheme (Scheme 4) the 2D-EXSY spectrum[18] (Figure 6) of the Pd complex **15** measured at −48 °C shows the interconversion of conformers A and C and the interconversion of conformers B and C. The direct degenerate interconversion of conformer C cannot be detected at −48 °C because the double-flip process is too slow at this temperature.

Because of the limited temperature range where kinetic line broadening effects are observable ($\Delta T = 24$ K for **15** and $\Delta T = 46$ K for **16**) and because of the small chemical shift differences of the exchanging sites ($\Delta\delta = 0.135$ ppm for **15** and $\Delta\delta = 0.168$ ppm for **16**), the analysis of the kinetic data is limited to the determination of the Gibbs free energy of activation $\Delta G^{\ddagger}$ by use of the Eyring equation ($\Delta G^{\ddagger} = -RT(\ln h/k_B + \ln k/T)$].[10] $\Delta G^{\ddagger}$ for the interconversion of A and C and of B and C by the rotation of one picoline ligand was found to be 12(±0.5) kcal/mol for the Pd compound **15** and 14(±0.5) kcal/mol for the Pt compound **16**. The variation of $\Delta G^{\ddagger}$ with temperature was found to be within the error limit.

The temperature-dependent line shapes of the ^{1}H NMR spectra of **15** and **16** obtained at 400 and 250 MHz are similar, and the kinetic analysis yielded comparable rate constants. As no variation of the spectra with solvent (CD_2Cl_2, CD_3OD) and concentration was found, a dissociative/associative exchange mechanism is not very likely.

Quantum-Chemical Calculations. To gain further insight into the bonding of the heterocyclic ligands to the metal and to support the different energy barriers found experimentally for the rotation around the Pd−N bond in complex **15** compared to the Pt−N bond in complex **16**, we performed *ab initio* calculations on the model complexes [dpe]Pd$(HNCH_2)_2^{2+}$ (**19**) and [dpe]Pt-$(HNCH_2)_2^{2+}$ (**20**) (dpe = diphosphinoethylene; see Figure 5 and Chart 3). The geometries of **19** and **20** were optimized at the HF/lanl2dz[17] level, and natural bond orbital (NBO) analyses[15] of the optimized structures were performed (Tables 1 and 2). The M−P and M−N bond lengths for **19** (M = Pd) and **20** (M = Pt) (Table 1) are similar and 0.05−0.03 Å shorter in the Pt compound **20**. Thus, the different energy barriers are likely not due to steric effects resulting from different M−P and M−N bond lengths in **15** and **16**. NBO analysis provides

(12) Perrin, D. D.; Armarego, W. L. F. *Purification of Laboratory Chemicals;* Pergamon Press: Oxford, U.K., 1988.
(13) (a) Schneider, H.-J.; Freitag, W. *J. Am. Chem. Soc.* **1976**, *98*, 978. (b) Siehl, H.-U.; Kaufmann, F. P.; Apeloig, Y.; Braude, V.; Danovich, D.; Berndt, A.; Stamatis, N. *Angew. Chem.* **1991**, *103*, 1546; *Angew. Chem., Int. Ed. Engl.* **1991**, *30*, 1479.
(14) Frisch, M. J.; Trucks, G. W.; Schlegel, H. B.; Gill, P. M. W.; Johnson, B. G.; Robb, M. A.; Cheeseman, J. R.; Keith, T.; Petersson, G. A.; Montgomery, J. A.; Raghavachari, K.; Al-Laham, M. A.; Zakrzewski, V. G.; Ortiz, J. V.; Foresman, J. B.; Cioslowski, J.; Stefanov, B. B.; Nanayakkara, A.; Challacombe, M.; Peng, C. Y.; Ayala, P. Y.; Chen, W.; Wong, M. W.; Andres, J. L.; Replogle, E. S.; Gomperts, R.; Martin, R. L.; Fox, D. J.; Binkley, J. S.; Defrees, D. J.; Baker, J.; Stewart, J. P.; Head-Gordon, M.; Gonzalez, C.; Pople, J. A. Gaussian 94, Revision E.1; Gaussian, Inc., Pittsburgh, PA, 1995.
(15) Reed, A. E.; Curtiss, L. A.; Weinhold, F. *Chem. Rev.* **1988**, *88*, 899. Reed, A. E.; Weinstock, R. B.; Weinhold, F. *J. Chem. Phys.* **1985**, *83*, 735.
(16) Wiberg, K. B. *Tetrahedron* **1968**, *24*, 1083.
(17) For a description of the lanl2dz basis set see: Hay, P. J.; Wadt, W. R. *J. Chem. Phys.* **1985**, *82*, 270, 284, 299.
(18) Jeener, J.; Meier, B. H.; Bachmann, P.; Ernst, R. R. *J. Chem. Phys.* **1979**, *71*, 4546−4563. Perrin, C. L.; Dwyer, T. J. *Chem. Rev.* **1990**, *90*, 935−967.

Scheme 4

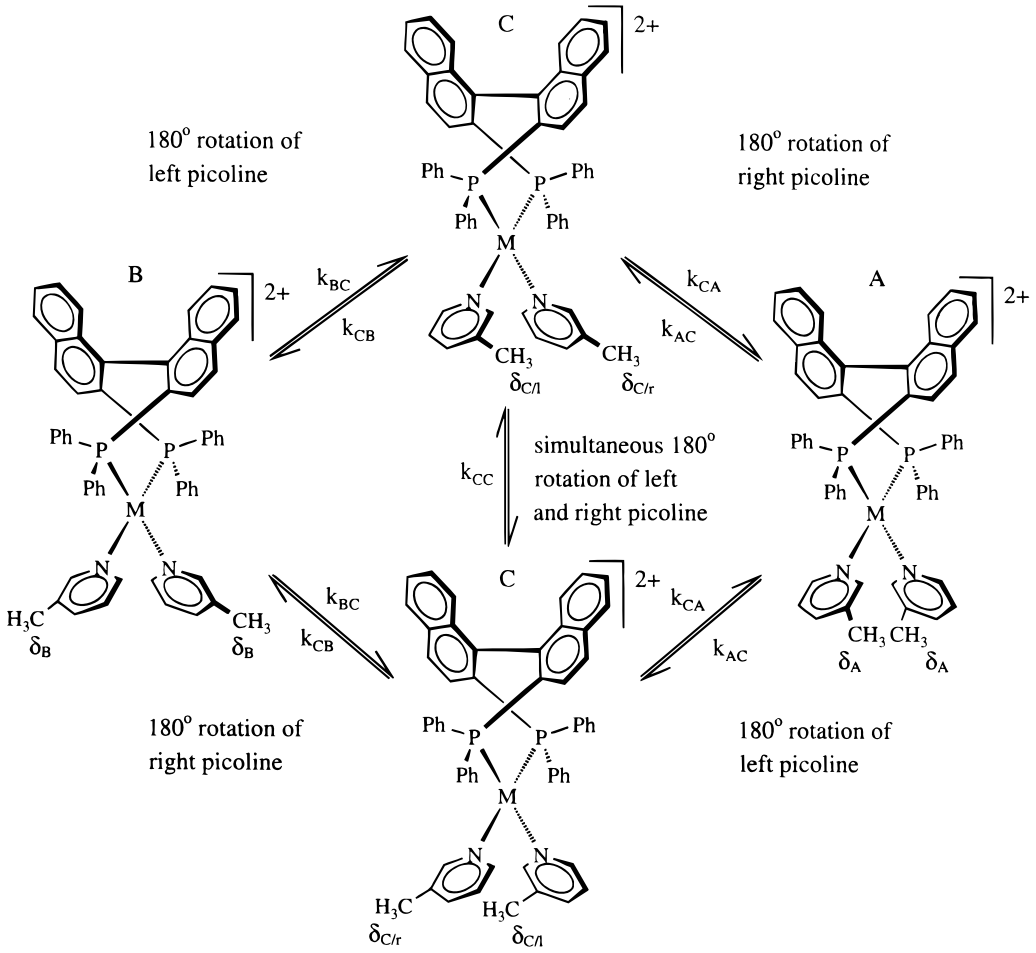

an interpretation of the geometric and electronic details of the model compounds in terms of Lewis structures in the parlance of VB-resonance theory. According to the NBO analysis, complexes **19** and **20** are best described by three resonance structures I−III, as shown in Chart 3. The "no bond" resonance structure I shows that there is no joint NBO of the metal and a nitrogen atom for **19** and **20**. Thus, according to the NBO analysis there is no standard two-center−two-electron bond between the metal and nitrogen. The bonding between the nitrogen and the metal atoms is obtained by delocalization of the electrons by the interaction of the NBO's of the metal and the nitrogen moieties. Resonance structure II (Chart 3) describes the shift of electron density from the lone electron pairs (LP) at nitrogen to the antibonding metal−phosphorus (M−P) σ-NBO's: LP(N^1)→BD*(M−P^1) and LP(N^2)→BD*(M−P^2) (Figure 5 and Table 2). This interaction is the main contribution to the bond energy of the nitrogen ligands to the metal and is much stronger for the Pt complex **20** (139.76 kcal/mol, Table 2) compared to the Pd complex **19** (97.81 kcal/mol, Table 2). This is in accord with the larger Wiberg bond index[16] of the M−N bonds for Pt complex **20** (0.322, Table 1) compared to Pd complex **19** (0.273, Table 1). Resonance structure III (Chart 3) describes the shift of electron density from the NC π-bonds to the antibonding M−P σ-NBO's: BD(N^1C)→BD*(M−P^1) and BD(N^2C)→BD*(M−P^2) (see Figure 5 and Table 2). The strength of this $\pi-\sigma$ interaction depends on the dihedral angle (H_2C−N−M−PH_2) formed by the atoms involved and thus also gives rise to a barrier for the rotation of the nitrogen ligands around the N−M linkage axis. This interaction is calculated to be stronger for the Pt complex **20** (5.54 kcal/mol, Table 2) than for the Pd complex **19** (2.68 kcal/mol, Table 2). This is in accord with the experimental observation that a higher energy barrier is observed for the rotation of the β-picoline ligands around the M−N linkage axis in the Pt complex **16** (14(±0.5) kcal/mol) than for the Pd complex **15** (12(±0.5) kcal/mol). The shift of electron density from the N−C π-bonds to the metal (resonance structure III, Chart 3) is more pronounced for the Pt complex **20** compared to the Pd complex **19**. Thus, the N−C bond distance is found to be longer in the Pt complex **20** (1.279 Å, Table 1) than in the Pd complex **19** (1.267 Å, Table 1). In accord with this, the Wiberg bond index of the N−C bond is 1.822 for the Pt complex **20** but 1.842 for the Pd complex **19** (Table 1).

Comparison of Rotational Barriers of Chiral BINAP Cationic Complexes with Covalent Systems. Despite the paucity of the data available on rotational barriers for Pt and Pd covalent complexes, several estimates can be found in the literature,[4] thus allowing us to build an interesting correlation between the relative bond strength and the value of the rotational barriers in chiral transition-metal bis(phosphanes). We found a free energy of activation to rotation of the β-picoline ligands of $\Delta G^{\ddagger} = 12(\pm 0.5)$ kcal/mol for the Pd(II) complex **15**. A somewhat higher barrier of 14(±0.5) kcal/mol is found in the cationic Pt(II) complex

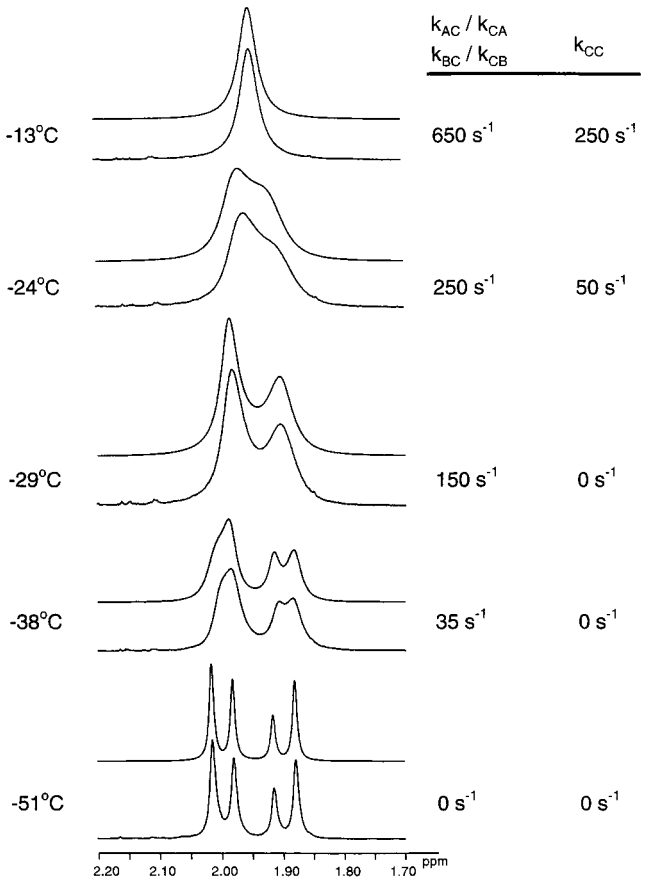

Figure 3. Experimental (lower traces) and simulated[8] (upper traces) 400 MHz ^{1}H NMR spectra of [BINAP]Pd(β-picoline)$_2$(OSO_2CF_3)$_2$ (**15**) at various temperatures with corresponding rate constants (see Scheme 4) of the rotation of the β-picoline ligands (solvent CD_3OD; δ(CHD_2OD) 3.31 ppm).

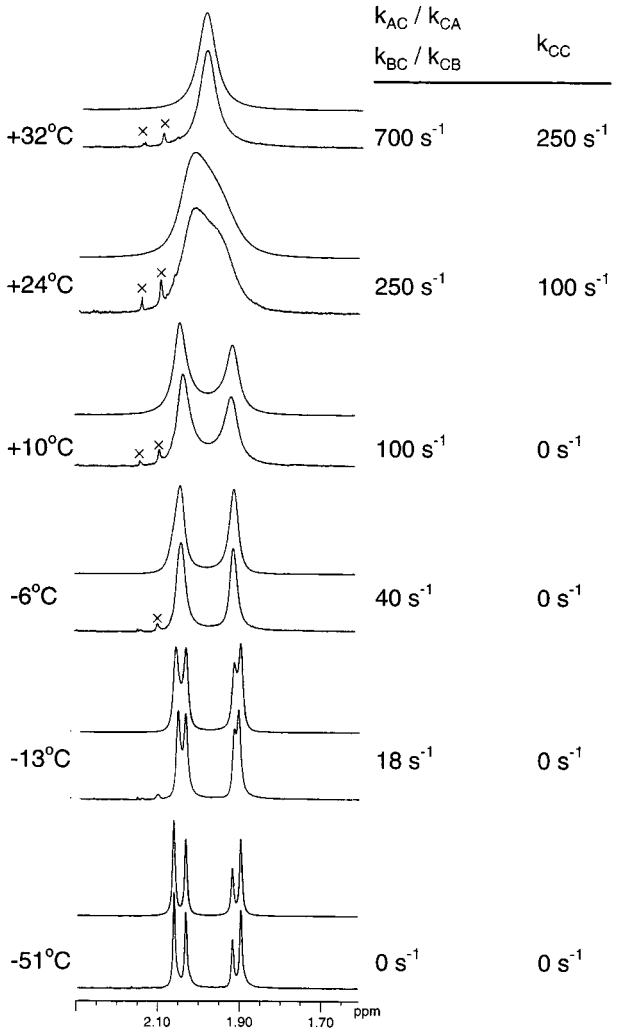

Figure 4. Experimental (lower traces) and simulated[8] (upper traces) 400 MHz ^{1}H NMR spectra of [BINAP]Pt(β-picoline)$_2$(OSO_2CF_3)$_2$ (**16**) at various temperatures with corresponding rate constants (see Scheme 4) of the rotation of the β-picoline ligands (solvent CD_3OD; δ(CHD_2OD) 3.31 ppm; × denotes impurities).

16. According to Brown and co-workers,[4] the chiral *covalent* BINAP *o*-anisole complex **8** has a barrier to rotation of 16.7 kcal/mol at 25 °C, as estimated by the line shape analysis with the DNMR3 program. The estimation of the rotational barrier for the covalent DIOP complex **7** provided a value for $\Delta G^{\ddagger}$ of at least 19 kcal/mol at 25 °C,[4] which is somewhat higher than for the BINAP complexes. These data are in good agreement with the trend discussed above derived from quantum-chemical calculations: the free energy of activation for the rotational barriers tends to increase with increasing strength of the metal−ligand bond. The M−N or M−C barriers are lowest for Pd−N complexes and higher for the complexes that contain Pt−C covalent bonds. The influence of steric factors is also important, as indicated by the comparison of the barriers for BINAP and DIOP complexes; therefore, the complexes with the larger bite angle tend to have higher activation barriers.

Conclusion

The interaction between chelated Pd(II) or Pt(II) triflates with various heteroaryl complexes results in the formation of diastereomeric, square-planar, cationic complexes. For reaction with [M(*R*-(+)-BINAP)[OTf]$_2$ (M = Pd, Pt) and 2-bromo-5-methylpyridine the formation of a diastereoisomeric mixture of three rotamers and a complex with a single heteroaryl group is observed. Reaction of 3-methylisoquinoline with the above bis(triflates) also yielded similar results, whereas in the case of the more sterically demanding 2-methylquinoline, exclusively the mono(heteroaryl) complexes [M(*R*-(+)-BINAP)(2-methylquinoline)][OTf]$_2$ (M = Pd, Pt) are observed. Steric effects of the substituents located in close proximity to the transition metal are found to be responsible for such remarkable control of the stoichiometry of the products. The observation of such a profound impact of the nearby located bromine or methyl group on the stoichiometry of the assembly is very interesting and important, as it permits introduction of different degrees of steric control on the formation of transition-metal-based complexes by simply varying the substituents at the α-position of the coodinated heteroaryl.

The restricted rotation about the metal−nitrogen heteroaryl bond in the complexes [Pd(*R*-(+)-BINAP)(3-picoline)$_2$][OTf]$_2$ and [Pt(*R*-(+)-BINAP)(3-picoline)$_2$]-[OTf]$_2$ was investigated by temperature-dependent ^{1}H NMR spectroscopy. The rotation barriers were determined by a kinetic line shape analysis of the methyl

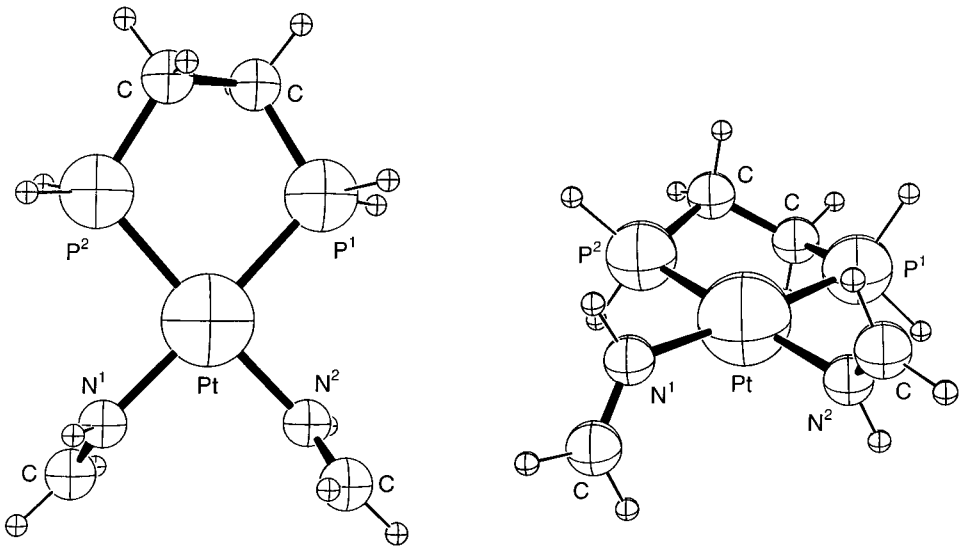

Figure 5. Optimized geometry (HF/lanl2dz) of model complex **20**.

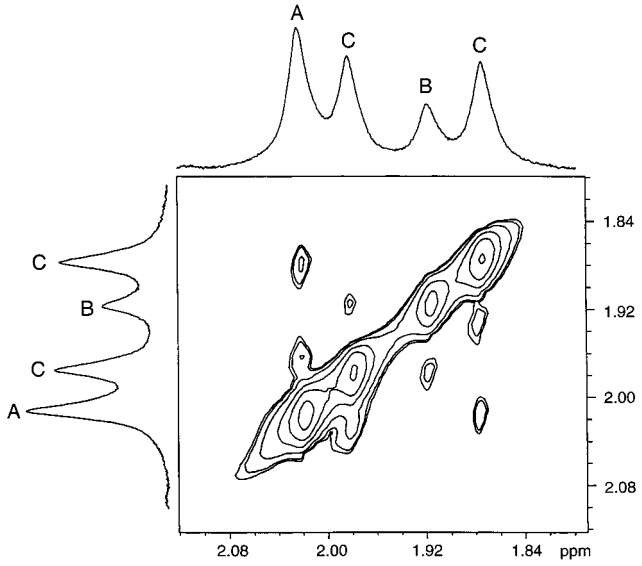

Figure 6. 500 MHz 2D-EXSY NMR spectrum of [BINAP]-Pd(β-picoline)$_2$(OSO_2CF_3)$_2$ (**15**) at −48 °C (mixing time 400 ms; solvent CD_3OD; $\delta(CHD_2OD)$ 3.31 ppm).

signals. The free energy of activation $\Delta G^{\ddagger}$ was found to be 12(±0.5) kcal/mol for the Pd complex **15** and 14(±0.5) kcal/mol for the Pt complex **16**.

Ab initio calculations (HF/lanl2dz) of model complexes [dpe]Pd(HN═CH_2)$_2^{2+}$ and [dpe]Pt(HN═CH_2)$_2^{2+}$ (dpe = diphosphinoethylene) support the interpretation of experimental results. The NBO analyses of the optimized structures show that the metal−nitrogen bonds are stronger for the Pt complex compared to the Pd complex. The interaction of the bonding N−C π-NBO's of the nitrogen ligands with the antibonding M−P σ-NBO's leads to hindered rotation around the nitrogen−metal bonds. The nitrogen−metal $\pi-\sigma$-interaction is found to be stronger for the Pt complex (M = Pt), resulting in a higher energy barrier for the rotation around the Pt−N bond compared to the rotation around the Pd−N bond.

These results represent the first attempt to address several important mechanistic points raised in our recent preliminary studies carried out with large chiral macromolecules.[2,3] (1) The rotation of the heteroaryl ligand is hindered, therefore making these assemblies

Chart 3. Resonance Structures of Model Complexes 19 (M = Pd) and 20 (M = Pt) according to the NBO Analysis of the *ab Initio* Optimized (HF/lanl2dz) Geometries

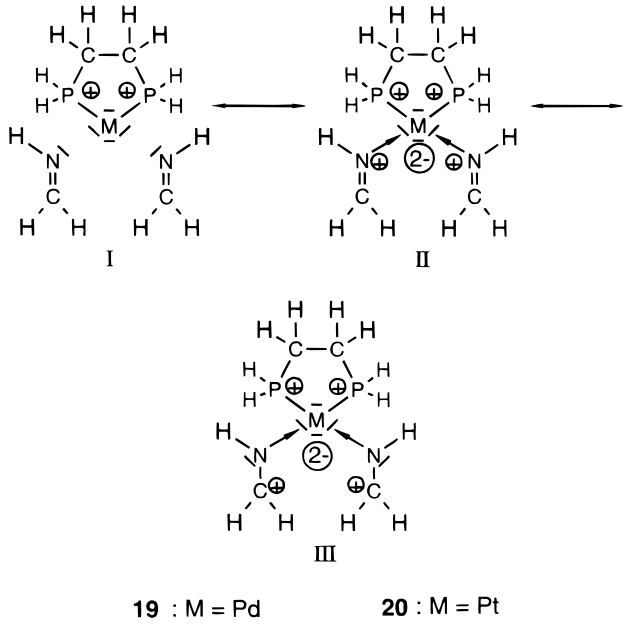

Table 1. *Ab Initio* Calculated (HF/lanl2dz) Bond Lengths (Å) and Wiberg Bond Indices of Model Complexes 19 (M = Pd) and 20 (M = Pt)[a]

	bond length		Wiberg bond index	
	19 (M = Pd)	**20** (M = Pt)	**19** (M = Pd)	**20** (M = Pt)
$MP^1 = MP^2$	2.486	2.432	0.480	0.545
$MN^1 = MN^2$	2.126	2.090	0.273	0.322
$N^1C = N^2C$	1.267	1.279	1.842	1.822
$P^1C = P^2C$	1.897	1.888	0.982	0.982
CC	1.538	1.539	1.046	1.045

[a] For numbering of the atoms, see Figure 5.

stable to interconversion even at elevated temperatures. Determination of the rotational barriers indicated that they are higher for Pt-containing assemblies as compared to their Pd counterparts. (2) Since these assemblies are formed in near-quantitative yield, it is easy to imply that there are some additional factors that

Table 2. Stabilization of Model Complexes 19 and 20 by the Interaction of NBO's[a]

	donor NBO→acceptor NBO	energy (kcal/mol)
19	$LP(N^1)\rightarrow BD^*(Pd-P^1)/LP(N^2)\rightarrow BD^*(Pd-P^2)$	97.81
20	$LP(N^1)\rightarrow BD^*(Pt-P^1)/LP(N^2)\rightarrow BD^*(Pt-P^2)$	139.76
19	$BD(N^1C)\rightarrow BD^*(Pd-P^1)/BD(N^2C)\rightarrow BD^*(Pd-P^2)$	2.68
20	$BD(N^1C)\rightarrow BD^*(Pt-P^1)/BD(N^2C)\rightarrow BD^*(Pt-P^2)$	5.54

[a] Geometries were calculated by the HF/lanl2dz method. See Figure 5 for numbering of the atoms. Definitions: LP(N), lone pair on nitrogen; BD(NC), bonding π-NBO of the nitrogen ligand; BD*(M−P), antibonding σ-NBO (M = Pd, Pt).

influence the formation and high thermodynamic stability of these macrocycles besides their conformational rigidity and the lability of the metal−heteroaryl bond. There are indirect indications that the degree of π-stacking between the phenyl ring of the bis(phosphane) (BINAP) and the coordinated heteroaryl plays an important role in the stabilization of these assemblies. A better understanding of these issues would provide a powerful strategy on how to use structural, stereochemical, and conformational effects in self-assembly to create complex stereochemically controlled entities with a large number of noncovalent interactions.

Experimental Section

General Methods. All reactions were conducted under a dry nitrogen atmosphere using Schlenk techniques, although the products can be handled in air. NMR spectra were recorded on a Varian XL-300 or Unity-300 spectrometer. ^{1}H NMR spectra were recorded at 300 MHz, and chemical shifts (δ) are reported in ppm relative to tetramethylsilane (Me_4Si) as an internal standard (0.0 ppm) or the proton resonance resulting from the incomplete deuteration of the NMR solvent: $CDHCl_2$ (5.32 ppm) or CHD_2OD (3.31 ppm). ^{13}C NMR spectra were recorded at 75 MHz, and chemical shifts (δ) are reported in ppm relative to the carbon resonance of the deuterated NMR solvent: CD_3OD (49.0 ppm) or CD_2Cl_2 (53.8 ppm). ^{31}P NMR spectra were recorded at 121 MHz, and chemical shifts (δ) are reported in ppm relative to external 85% H_3PO_4 at 0.00 ppm. ^{19}F NMR spectra were recorded at 282 MHz, and chemical shifts are reported relative to external $CFCl_3$ at 0.00 ppm.

Temperature-dependent ^{1}H NMR spectra of complexes **15** and **16** were recorded at 400 MHz on a Bruker ARX 400 NMR spectrometer and at 250 MHz on a Bruker ARX 250 NMR spectrometer. The chemical shifts are reported relative to the residual signals of incompletely deuterated solvent CHD_2OD (3.31 ppm). The probe temperature was calibrated with a ^{13}C chemical shift thermometer using neat 2-chlorobutane.[13]

The rate constants were determined from the NMR spectra by line shape analysis using the WIN-DYNAMICS program.[8] The assumption was made that the interconversions of A and C and of B and C by the rotation of one β-picoline ligand have the same rate constant at a given temperature ($k_{AC} = k_{CA} = k_{BC} = k_{CB}$). The populations of the conformers A−C at different temperatures were adjusted to give the best fit to the experimental spectra. The Gibbs free energy of activation was calculated using the Eyring equation ($\Delta G^{\ddagger} = -RT(\ln h/k_B + \ln k/T)$).[10] The error[10] in $\Delta G^{\ddagger}$ ($\Delta\Delta G^{\ddagger}$) was calculated as $\Delta\Delta G^{\ddagger} = RT\{[\Delta T/T(\ln k_B T/hk + 1)]^2 + (\Delta k/k)^2\}^{1/2}$ with a determination uncertainty of the temperature of $\Delta T = 3$ K and a relative determination uncertainty of the rate constants of $\Delta k/k = 0.1$.

IR spectra were recorded on a Mattson Polaris FT-IR spectrophotometer. Microanalyses were performed by Atlantic Microlab Inc., Norcross, GA. Melting points were obtained with a Mel-Temp capillary melting point apparatus and are not corrected. Abbreviations: br, broad; m, multiplet; s, singlet; d, doublet; isoq, isoquinoline; quin, quinoline; 3-Brpy, 3-bromopyridine; H_o, ortho proton; H_m, meta proton; H_p, para proton, Isomer A denotes the diastereomer or NMR-equivalent enantiomeric pair that is present in the greater amount, whereas isomer B refers to the diastereomer or NMR-equivalent enantiomeric pair that is present in the smaller amount, as indicated by the peak ratios in the ^{1}H and ^{31}P NMR. Isomer C indicates an asymmetrical *syn* isomer in chiral bis(phosphane) complexes.

Quantum-chemical calculations were performed with the Gaussian 94 program suite[14] using SGI (Indigo 2, R 8000) and Sun-Enterprise (E4000, Ultrasparc 250 MHz) hardware.

Materials. Solvents were purified as follows: CH_2Cl_2 and $CHCl_3$ were purified by literature procedures[12] and distilled over CaH_2; Et_2O was purified by literature procedures[12] and distilled over Na/benzophenone; CD_2Cl_2 was vacuum-transferred from CaH_2. As a precaution, all solvents were freeze−thaw−pump degassed twice before use.

All commercial reagents were ACS reagent grade. 3-Bromopyridine, isoquinoline, quinoline, silver triflate, *R*-(+)-2,2′-bis(diphenylphosphino)-1,1′-binaphthyl (*R*-(+)-BINAP), and [Pd(*R*-(+)-BINAP)][Cl]$_2$ were all obtained from Aldrich and used as received. The precursors [Pd(*R*-(+)-BINAP)(H_2O)][OTf]$_2$ (**9**) and [Pt(*R*-(+)-BINAP)(H_2O)][OTf]$_2$ **(10)** were prepared by a literature procedure.[7]

Reaction of [Pd(*R*-(+)-BINAP)][OTf]$_2$ with 2-Bromo-5-methylpyridine (11). A 25 mL Schlenk flask equipped with a stir bar was charged with 28.7 mg (0.167 mmol) of 2-bromo-5-methylpyridine and CH_2Cl_2 (5 mL). To this was added 70.2 mg (0.067 mmol) of Pd(*R*-(+)-BINAP)(H_2O)(OTf)$_2$, and the resulting solution was stirred under nitrogen for 10 min at ambient temperature. The solution was transferred *via* syringe into a 50 mL flask and reduced in volume to *ca*. 2 mL *in vacuo*. Diethyl ether was added, and the white precipitate was collected and washed with diethyl ether and dried *in vacuo*: yield of **11** 79.7 mg (86%) of a *ca*. 1:1 ratio of disubstituted and monosubstituted products (by NMR); mp 172 °C. No decomposition was observed upon melting. ^{1}H NMR (CD_2Cl_2): low field, 10.23 (s, *anti* isomer B), 9.97 (s), 9.95 (s) (*syn* isomer A), 9.93 (*anti* isomer C), 9.41 (mono isomer D); high field, 2,98 (s, *anti* isomer B), 2.87 (s, mono-isomer D), 2.76 (s, *syn* isomer A), 2.60 (s, *anti* isomer C), 2.49 (s, *syn* isomer A). ^{31}P{^{1}H} NMR (CD_2Cl_2): 32.32 (s, mono isomer), 25.34 (s, *anti* isomer C), 23.91 (s, *anti* isomer B), 24.65 (d, $J = 21$ Hz, *syn* isomer A, P′), 22.18 (d, $J = 21$ Hz, *syn* isomer A, P″). ^{19}F NMR (CD_2Cl_2): −76.11 (s, 2 CF_3SO_3). Anal. Calcd for $C_{58}H_{44}N_2P_2S_2F_6O_6Br_2Pd$ (disubstituted) + $C_{52}H_{38}NP_2S_2F_6O_6BrPd\cdot H_2O$ (monosubstituted): C, 51.04; H, 3.27; N, 1.62; S, 4.96; Br, 9.26. Found: C, 51.14; H, 3.52; N, 1.58; S, 4.79, Br, 8.98. Attempts to separate the four different isomers were unsuccessful.

Reaction of [Pt(*R*-(+)-BINAP)][OTf]$_2$ with 2-Bromo-5-methylpyridine (12). A 50 mL Schlenk flask equipped with a stir bar was charged with 22.8 mg (0.133 mmol) of 2-bromo-5-methylpyridine and CH_2Cl_2 (5 mL). Pt(*R*-(+)-BINAP)(H_2O)(OTf)$_2$ (60.0 mg; 0.053 mmol) was added, and the resulting mixture was stirred under nitrogen for 20 min at ambient temperature. The solution was transferred *via* syringe into a 50 mL flask and reduced in volume to *ca*. 2 mL on a rotary evaporator. Diethyl ether was added, and the white precipitate was collected and washed with diethyl ether and dried *in vacuo*. The disubstituted products can be separated from the monosubstituted one by fractional crystallization from CH_2Cl_2−diethyl ether: yield of **12** 65.0 mg (83%); yield of disubstituted stereoisomers **12a**−**c** 25.0 mg (32%); mp 210 °C. ^{1}H NMR (CD_2Cl_2): low-field, 9.19 (s, *anti* isomer B), 9.11 (s), 8.95 (s) (both of *syn* isomer A), 8.71 (bs, *anti* isomer C); high-field, 2,36 (s, *anti* isomer B), 2.33 (s, *anti* isomer C), 2.28 (s), 2.08 (s) (both of *syn* isomer A). ^{31}P{^{1}H} NMR (CD_2Cl_2): −0.806 (s, ^{195}Pt satellites $J_{Pt-P} = 3405$, *anti* isomer B), −2.22 (d, $J = 26$ Hz, *syn* isomer A, P′), −4.24 (d, $J = 26$ Hz, *syn* isomer A, P″), −4.26 (s, *anti* isomer C), 23.91 (s). ^{19}F NMR (CD_2Cl_2): −74.57 (s, 2 CF_3SO_3). IR (neat, cm^{-1}): 1276, 1223, 1099, 1031 (all OTf).

Anal. Calcd for $C_{58}H_{44}N_2P_2S_2F_6O_6Br_2Pt\cdot H_2O$: C, 47.13; H, 3.14; N, 1.90; S, 4.34; Br, 10.81. Found: C, 47.43; H, 3.18; N, 1.76; S, 4.31; Br, 10.00.

[Pd(*R*-(+)-BINAP)(2-methylquinoline)][OTf]$_2$ (13). A 20 mL Schlenk flask was charged with 25.2 mg (0.176 mmol) of 2-methylquinoline and CH_2Cl_2 (5 mL). Pd(*R*-(+)-BINAP)(H_2O)-($OTf)_2$ (68.7 mg; 0.066 mmol) was added, and the resulting colorless mixture was stirred under nitrogen for 0.5 h at ambient temperature. The solution was transferred into a 50 mL flask and reduced in volume to *ca*. 2 mL. Diethyl ether was then added, resulting in the formation of a precipitate, which was collected, washed with diethyl ether (5 mL), and dried *in vacuo*: yield of **13** 65.4 mg (76%); mp 144−148 °C dec. ^{1}H NMR (CD_2Cl_2): 8.81 (d, J = 9.0 Hz, 1H, quin), 8.45 (d, J = 8.9 Hz, 1H, quin), 8.12 (d, J = 8.8 Hz, 1H, quin), 8.08 (t, J = 7.1 Hz, 1H, quin), 7.68 (m, 12H, overlap of BINAP and quin signals), 7.44 (m, 8H, BINAP), 7.12 (m, 12H, BINAP), 6.55 (d, J = 8.6 Hz, 2H, BINAP), 3.08 (s, 3H, quin CH_3). ^{13}C-{^{1}H} NMR (CD_2Cl_2): 146.4, 139.1, 135.4 (quin), 135.0, 134.5, 133.3, 132.3, 132.0, 130.4, 130.1, 129.3, 129.2, 129.0, 128.8, 128.7, 127.6, 127.3, 127.0, 125.5 (BINAP and quin), 124.8 (C_i, BINAP), 123.9 (BINAP), 123.5 (quin), 121.2, 121.0 (q, OTf, J_{C-F} = 318 Hz), 120.2, 129.3 (BINAP), 21.3 (quin CH_3). ^{31}P{^{1}H} NMR (CD_2Cl_2): 32.4 (s). ^{19}F NMR (CD_2Cl_2): −74.6 (s, 2 CF_3-SO_3). IR (neat, cm^{-1}): 1255, 1171, 1031 (all OTf). Anal. Calcd for $C_{56}H_{41}NP_2S_2F_6O_6Pd\cdot 2H_2O$: C, 55.75; H, 3.76; N, 1.16; S, 5.32. Found: C, 55.53; H, 3.70; N, 1.23; S, 5.29.

[Pt(*R*-(+)-BINAP)(2-methylquinoline)][OTf]$_2$ (14). A 20 mL Schlenk flask equipped with a stir bar was charged with 20.0 mg (0.139 mmol) of isoquinoline, 5 mL of CH_2Cl_2, and 60.0 mg (0.053 mmol) of Pt(*R*-(+)-BINAP)(H_2O)($OTf)_2$. The resulting mixture was stirred under nitrogen for 0.5 h at ambient temperature. The solution was then transferred *via* syringe into a 50 mL flask and reduced in volume to 5 mL *in vacuo*. Diethyl ether was added, resulting in the formation of a white precipitate, which was collected and washed with diethyl ether and dried *in vacuo*: yield of **14** 62.0 mg (82%); mp 154−158 °C dec. ^{1}H NMR (CD_2Cl_2): 8.79 (d, J = 8.7 Hz, 1H, quin), 8.45 (d, J = 8.6 Hz, 1H, quin), 8.14 (d, J = 8.4 Hz, 1H, quin), 8.01 (t, J = 7.3 Hz, 1H, quin), 7.87 (t, J = 7.2 Hz, 1H, quin), 7.74 (d, J = 8.4 Hz, 2H, BINAP), 7.67 (m, 6H, BINAP), 7.51−7.39 (m, 11H, BINAP + quin), 7.12 (br s, 8H, BINAP), 7.07−6.94 (m, 4H, BINAP), 6.54 (d, J = 8.9 Hz, 2H) (BINAP), 3.04 (s, 3H, quin CH_3). ^{13}C{^{1}H} NMR (CD_2Cl_2): 146.1, 139.2, 135.4 (quin), 135.0, 134.8, 134.6, 134.1, 133.2, 132.3, 131.8, 130.3, 130.0, 129.1, 128.9, 128.7, 127.53, 127.45, 126.6, 124.4 (BINAP and quin), 123.4, 122.2 (BINAP), 123.5 (quin), 121.5, 121.0 (q, OTf, J_{C-F} = 322 Hz), 119.9, 119.1 (BINAP), 21.5 (quin CH_3). ^{31}P{^{1}H} NMR (CD_2Cl_2): 4.69 (s, ^{195}Pt satellites, J_{Pt-P} = 3670 Hz). ^{19}F NMR (CD_2Cl_2): −77.6 (s, 2 CF_3-SO_3). IR (neat, cm^{-1}): 1223, 1156, 1030 (all OTf). Anal. Calcd for $C_{56}H_{41}NP_2S_2F_6O_6Pt\cdot 2H_2O$: C, 51.93; H, 3.50; N, 1.08; S, 4.95. Found: C, 51.90; H, 3.36; N, 1.19; S, 4.94.

[Pd(*R*-(+)-BINAP)(3-picoline)$_2$][OTf]$_2$ (15). A 10 mL Schlenk flask equipped with a stir bar was charged with 15.5 mg (0.166 mmol) of 3-picoline and 3 mL of CH_2Cl_2. A solution of 52.3 mg (0.050 mmol) of Pd(*R*-(+)-BINAP)(H_2O)($OTf)_2$ in 1 mL of CH_2Cl_2 was added, and the resulting solution was stirred under nitrogen for 10 min at ambient temperature. Slow addition of a diethyl ether−pentane (1:5) mixture afforded the product as a precipitate, which was collected and washed with a minimum of diethyl ether−pentane: yield of **15** 47.0 mg (78%); mp 272−274 °C dec. ^{1}H NMR (CD_2Cl_2): 8.70 (br s, 2H, py), 8.56 (bd, 4H, py), 8.17 (t, J = 9.0 Hz, 2H), 8.03 (d, J = 9.0, 2H), 7.94 (m, 8H), 7.86 (d, J = 8.0 Hz, 2H), 7.60 (t, 2H, J = 7.8 Hz), 7.45 (s, 8H) (all BINAP), 7.32 (s, 2H, J = 7.8 Hz, py), 7.17 (m, 4H, BINAP + py), 6.98 (t, J = 5.9 Hz, 2H), 6.55 (d, J = 8.4 Hz, 2H) (BINAP), 2.15 (s, 6H, py CH_3). ^{13}C-{^{1}H} NMR (CD_2Cl_2): 151.9, 148.7, 139.7 (py), 136.9, 135.2, 135.1, 133.5, 131.9, 130.5, 129.9, 129.1, 129.0, 128.9, 127.6, 127.7, 127.4, 127.2, 125.5 (BINAP and py), 125.2 (C_i, BINAP), 124.4 (BINAP), 124.3 (py), 121.5 (q, OTf, J_{C-F} = 320 Hz), 119.8, 119.0 (BINAP), 18.1 (py CH_3). ^{31}P{^{1}H} NMR (CD_2Cl_2): 25.4 (s). ^{19}F NMR (CD_2Cl_2): −77.5 (s, 2 CF_3SO_3). IR (neat, cm^{-1}): 1254, 1153, 1030 (all OTf). Anal. Calcd for $C_{58}H_{46}N_2P_2S_2F_6O_6$-$Pd\cdot H_2O$: C, 56.57; H, 3.93; N, 2.27; S, 5.21. Found: C, 56.40; H, 3.78; N, 2.28; S, 5.21.

[Pt(*R*-(+)-BINAP)(3-picoline)$_2$][OTf]$_2$ (16). A 10 mL Schlenk flask equipped with a stir bar was charged with 18.5 mg (0.199 mmol) of 3-picoline and CH_2Cl_2 (1 mL). A colorless solution of 57.0 mg (0.050 mmol) of Pt(*R*-(+)-BINAP)(H_2O)-($OTf)_2$ in 1 mL of CH_2Cl_2 was added, and the reaction mixture was stirred under nitrogen for 4.5 h at room temperature. A diethyl ether−pentane mixture was added, and the product was collected and washed with diethyl ether−pentane and dried *in vacuo*: yield of **16** 52.6 mg (79%); mp 248−252 °C (the compound gradually decomposed at temperatures above 220 °C). ^{1}H NMR (CD_2Cl_2): 8.71 (br s, 2H, py, isomer B + A), 8.60 (br s, 2H, py, isomer C), 8.46 (br d, 4H, py), 7.98 (t, 2H), 7.95 (d, 2H), 7.74 (m, 8H), 7.69 (d, J = 8.2 Hz, 2H), 7.40 (t, 2H, J = 7.8 Hz), 7.31 (s, 8H) (all BINAP), 7.20 (s, 2H, J = 7.8 Hz, py), 7.01 (m, 4H, BINAP + py), 6.88 (t, J = 5.9 Hz, 2H), 6.43 (d, J = 8.4 Hz, 2H, isomer C), 6.36 (d, J = 8.0 Hz, 2H, isomers A + B) (BINAP), 2.05 (s, 6H, py CH_3, isomers A + B), 1.98 (s, 6H, py CH_3, isomer C). ^{13}C{^{1}H} NMR (CD_2Cl_2): 151.1 (isomer A), 151.9 (isomer B), 151.8 (isomer C), 148.9, 140.3 (py), 136.9, 135.2, 134.8, 133.4, 132.3, 131.9, 131.7, 130.3, 128.8, 128.6, 127.5, 127.4, 127.3, 127.2, 127.1, 126.0 (BINAP and py), 125.2, 123.8 (BINAP), 124.3 (py), 121.4 (q, OTf, J_{C-F} = 319 Hz), 119.5, 119.2 (BINAP), 18.1 (py CH_3). ^{31}P{^{1}H} NMR (CD_2Cl_2): 0.72 (s, ^{195}Pt satellites, $^1J_{P-Pt}$ = 3275 Hz, isomer C), 1.21 (d, J = 24 Hz, ^{195}Pt satellites, $^1J_{P-Pt}$ = 3275 Hz, isomer B), −0.12 (d, J = 24 Hz, ^{195}Pt satellites, $^1J_{P-Pt}$ = 3275 Hz, isomer B), 0.11 (s, ^{195}Pt satellites, $^1J_{P-Pt}$ = 3275 Hz, isomer A). ^{19}F NMR (CD_2Cl_2): −77.5 (s, 2 CF_3SO_3). IR (neat, cm^{-1}): 1258, 1224, 1156, 1031 (all OTf). Anal. Calcd for $C_{58}H_{46}N_2P_2S_2$-$F_6O_6Pt\cdot 2H_2O$: C, 52.06; H, 3.77; N, 2.09; S, 4.79. Found: C, 52.06; H, 3.59; N, 2.01; S, 4.81.

Reaction of [Pd(*R*-(+)-BINAP)][OTf]$_2$ with 3-Methylisoquinoline. Compound 17. A 20 mL Schlenk flask equipped with a stir bar was charged with 24.0 mg (0.168 mmol) of 3-methylisoquinoline and CH_2Cl_2 (5 mL). Then, 70.2 mg (0.067 mmol) of Pd(*R*-(+)-BINAP)(H_2O)($OTf)_2$ was added, and the resulting mixture was stirred under nitrogen for 0.5 h at ambient temperature. To this solution was added a pentane−diethyl ether mixture, resulting in the formation of a white precipitate, which was collected and washed with 5 mL of pentane and dried *in vacuo*: yield of **17** 80.6 mg (91%); mp 198−203 °C dec. ^{31}P{^{1}H} NMR (CD_2Cl_2): 25.90 (d, J = 13 Hz, *syn* isomer C, P′), 25.78 (s, *anti* isomer A), 24.53 (s, *anti* isomer C), 22.81 (d, J = 13 Hz, *syn* isomer C, P″). Anal. Calcd for a 1:1 ratio of $C_{66}H_{50}N_2P_2S_2F_6O_6Pd$ (disubstituted) + $C_{56}H_{41}$-$NP_2S_2F_6O_6Pd\cdot H_2O$ (monosubstituted): C, 58.56; H, 3.75; N, 1.68; S, 5.13. Found: C, 58.96; H, 3.89; N, 2.02; S, 4.77. Attempts to separate different isomers of **17** were unsuccessful.

Reaction of [Pt(*R*-(+)-BINAP)][OTf]$_2$ with 3-Methylisoquinoline. Mono(heteroaryl) Compound 18d. To a solution of 18.9 mg (0.132 mmol) of 3-methylisoquinoline and 5 mL of CH_2Cl_2 in a 20 mL Schlenk flask was added 60.0 mg (0.053 mmol) of Pt(*R*-(+)-BINAP)(H_2O)($OTf)_2$ *via* syringe, and the resulting mixture was stirred under nitrogen for 0.5 h at ambient temperature. The clear solution was transferred *via* syringe into a 50 mL flask and reduced in volume to *ca*. 1 mL on rotary evaporator. A diethyl ether−pentane mixture was added, resulting in the formation of a white precipitate, which was collected and washed with pentane. The white microcrystalline product was dried *in vacuo*: yield of **18** 57.0 mg (75%). The analytically pure compound **18d** was obtained by recrystallization of the product from a pentane−CH_2Cl_2 mixture: mp 168−174 °C dec. ^{1}H NMR (CD_2Cl_2): 9.41 (s, 1H, isoquin), 8.15 (d, J = 8.3 Hz, 1H, isoquin), 7.90 (d, J = 3.8 Hz, 1H, isoquin), 7.81 (s, 1H, isoquin), 7.77−7.63 (m, 11H, BINAP

+ isoquin), 7.55−7.28 (m, 10H, BINAP), 7.12 (bs, 8H, BINAP), 7.07−6.80 (m, 4H, BINAP), 6.53 (d, J = 8.7 Hz, 2H) (BINAP), 2.84 (s, 3H, isoquin CH_3). $^{31}P\{^1H\}$ NMR (CD_2Cl_2): 5.06 (s, ^{195}Pt satellites, J_{Pt-P} = 3668 Hz). ^{19}F NMR (CD_2Cl_2): −77.6 (s, 2 CF_3SO_3). IR (neat, cm^{-1}): 1224, 1154, 1030 (all OTf). Anal. Calcd for $C_{56}H_{41}NP_2S_2F_6O_6Pt\cdot H_2O$: C, 52.67; H, 3.39; N, 1.10; S, 5.02. Found: C, 52.87; H, 3.50; N, 1.41; S, 4.85.

Acknowledgment. A University of Utah Graduate Dissertation Fellowship to Bogdan Olenyuk is gratefully acknowledged. We also thank the National Science Foundation (Grant No. CHE-9529093) and the Fond der Chemischen Industrie for financial support as well as Johnson-Matthey for a generous loan of platinum salts. We thank Thomas Nau, Computer Center, University of Ulm, Ulm, Germany, for software adaptations and Herbert Thiele, Bruker Franzen Analytic GmbH, Bremen, Germany, for a prerelease version of the Bruker WinNMR program suite. We acknowledge useful comments of one of the reviewers.

Supporting Information Available: Proton, ^{31}P, and ^{13}C NMR and IR spectra of compounds **11**−**18**. This material is available free of charge via the Internet at http://pubs.acs.org.

OM9803927